



Microstructure and deformation behavior of Cu–Zn–Al–(Si) shape memory alloys under quenching controlled from the α/β phase region

Atik Setyani^{1,*}, Hendy Roesma Wardhana¹, Nur Amin²,
Ignatius Andre Setiawan³, Nina Fapari Arif⁴

¹Metallurgical Engineering, Universitas Pembangunan Nasional Veteran Yogyakarta, Yogyakarta 55281, Indonesia

²Mechanical Engineering, Universitas Diponegoro, Semarang 50275, Indonesia.

³Faculty of Engineering Technology, University of Twente, Enschede 7500, Netherlands

⁴Management, Universitas Pembangunan Nasional Veteran Yogyakarta, Yogyakarta 55283, Indonesia

*Corresponding author: atik.setyani@upnyk.ac.id

Abstract

Shape Memory Alloys (SMAs) are functional materials with rapidly expanding applications in medical devices, aerospace, and smart actuators. Among them, Cu–Zn–Al-based SMAs are cost-effective but their performance is often limited by the formation of non-reversible martensite. This study investigates the influence of Si addition and quenching methods on the microstructure, martensitic transformation, and deformation behavior of Cu–Zn–Al SMAs. Alloys with compositions of Cu–27Zn–2.5Al and Cu–27Zn–2.5Al–0.3Si wt.% were fabricated via gravity casting and homogenized at 850°C for 2 hours. The samples were then beta-tized at 900°C for 30 minutes and cooled using two quenching methods: Direct Quenching (DQ) and Up Quenching (UQ). The UQ process involved reheating after initial quenching to promote atomic ordering and defect relaxation, followed by cooling in an ethanol+dry ice mixture maintained at –5°C. The results reveal that the Cu–27Zn–2.5Al wt.% alloy undergoes a $\beta \rightarrow \beta'$ martensitic transformation in both DQ and UQ conditions, with UQ producing a more homogeneous and responsive martensitic structure. In contrast, the addition of 0.3 wt.% Si refines the α -phase grains and stabilizes the $\alpha + \beta$ phase region, thereby suppressing martensite formation. The Si-containing alloy deforms mainly through plastic slip in the α phase, whereas the Si-free alloy exhibits the typical twinning/detwinning mechanism of SMAs. These findings confirm that the combination of alloy composition and quenching route governs phase transformation and deformation mechanisms in Cu-based SMAs, offering insight for designing low-cost functional materials with tunable shape memory behavior.

Keywords:

Deformation, phase transformation, quenching, shape memory alloy.

1 Introduction

Shape Memory Alloys (SMAs) are functional materials currently experiencing a significant increase in market value due to their wide-ranging applications in the medical field, transportation, aerospace, and smart actuator devices [1-3]. Cu-based systems, especially Cu–Zn–Al, are an attractive alternative to SMAs because of their low production cost, ease of fabrication, and good shape memory properties at various temperatures [4]. The shape memory effect in these alloys is controlled by the nondiffusional transformation of the β phase into β' martensite. The presence of

the α phase enhances mechanical strength, but it has the potential to reduce the homogeneity of the martensitic transformation [4]. Therefore, controlling the proportion of α and β phases is a crucial strategy for balancing mechanical and functional properties.

Improving the performance of Cu–Zn–Al is attainable through compositional modifications or heat treatment processes [5, 6]. The addition of silicon (Si) is known to form intermetallic precipitates, increase hardness, and modify the kinetics of martensitic transformation [7]. However, studies on the effect of Si on the stability of the α/β phase and thermoelastic deformation behavior in Cu–Zn–Al are still limited, so further research is needed. In addition, the quenching method also plays a crucial role in determining the phase morphology [8]. Direct Quench (DQ) results in rapid cooling from a high temperature but tends to induce crystal defects and stabilization of metastable martensite, which reduces the shape memory effect [9-11]. Therefore, a post-treatment is needed to improve crystal ordering and reduce defects to optimize the shape memory properties.

Previous studies on Cu–Zn–Al-based shape memory alloys have mainly focused on composition optimization and conventional quenching techniques to enhance the shape memory effect. However, these approaches often lead to issues such as metastable martensite formation, poor thermo-elastic reversibility, and microstructural inhomogeneity, particularly when rapid quenching media like liquid nitrogen are employed. Moreover, the role of Si as a phase stabilizer and its interaction with different quenching routes in influencing martensitic transformation behavior remains insufficiently explored. In this study, the Up-Quench (UQ) approach is used as a post-treatment strategy with the potential to eliminate martensite stabilization and enhance thermoelastic transformation capability. The UQ method includes a controlled reheating step after quenching, which promotes atomic reordering and relaxation of crystal defects, thereby enhancing reversibility during phase transformation. Another novelty of this research is the use of a cooling medium consisting of alcohol combined with dry ice, which offers a high cooling rate, reaches a low temperature, and is more economical and safer than liquid nitrogen, which has a very low temperature and often results in cracking of the material. The research focuses on Cu–Zn–Al and Cu–Zn–Al–Si alloys in the $\alpha+\beta$ region to evaluate the effect of various quenching methods on microstructure evolution, phase transformation, and thermoelastic deformation behavior. With this approach, the research is expected to provide a fundamental understanding of the role of Si and the UQ method in optimizing reversible martensitic transformation in copper-based SMAs.

2 Research methodology

2.1 Alloy fabrication

The overall fabrication and heat treatment procedures of the Cu–27Zn–2.5Al wt.% and Cu–27Zn–2.5Al–0.3Si wt.% alloys are illustrated in Fig. 1. As shown in Fig. 1, the fabrication process begins with the melting of high-purity raw materials (99.9% pure Cu, Al, and Zn ingots) using an induction furnace. Copper is melted first, followed sequentially by aluminum and zinc, to accommodate the differences in their melting temperatures. Prior to casting, the steel mold was preheated to approximately 800°C to prevent thermal shock and ensure uniform solidification. The molten alloy was then poured into the preheated mold at approximately 1150°C, forming an ingot with dimensions of 110×110×6 mm.

Plat as cast involves homogenization at 850°C for 2 h and beta-tizing at 900°C for 30 min, followed by quenching using either the DQ or UQ method. Homogenization is intended to eliminate chemical segregation produced during the solidification of the as-cast alloy.

2.2 Homogenization and heat treatment

All as-cast samples were homogenized at 850°C for 2 hours, then air-cooled to eliminate chemical segregation formed during the

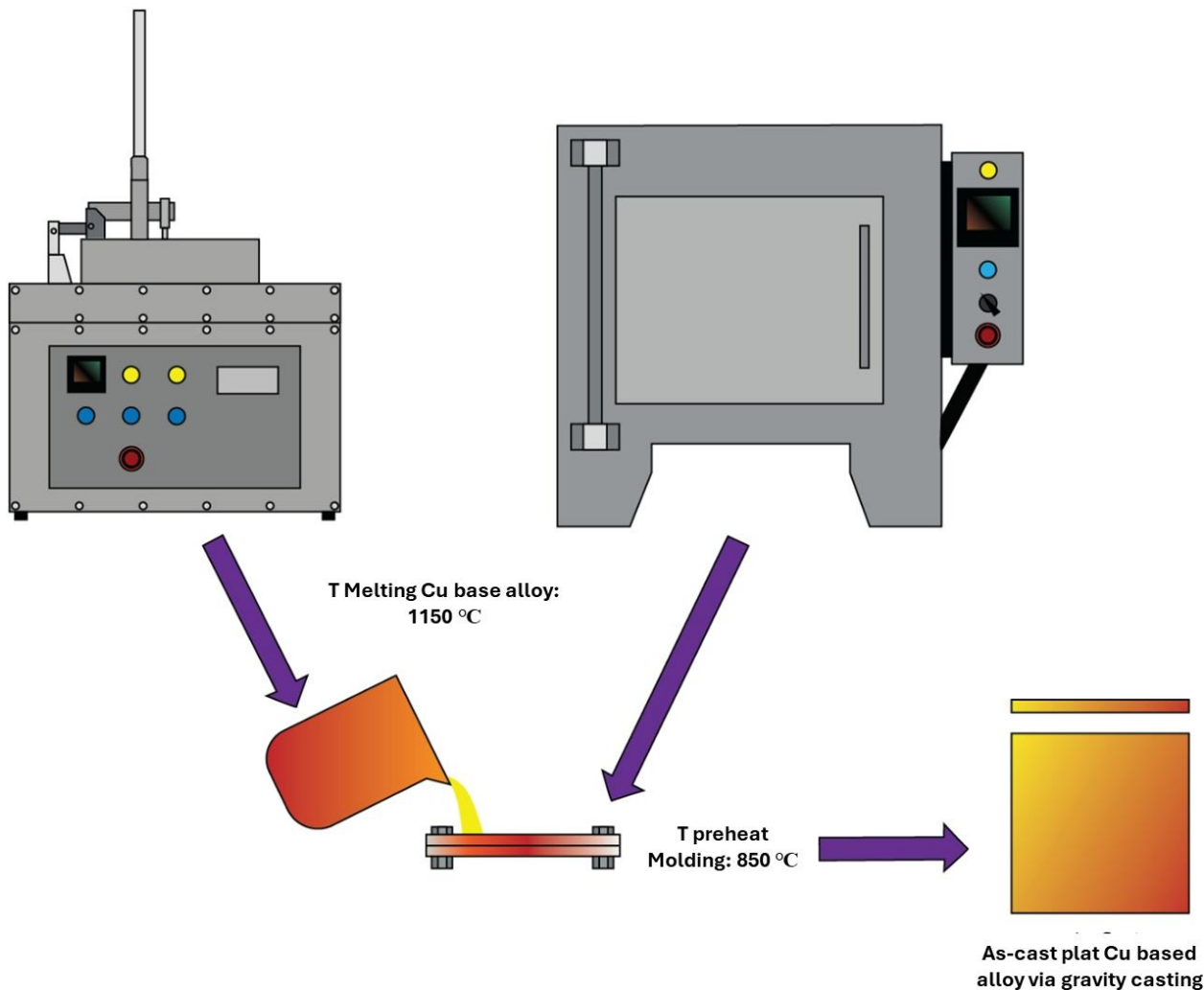


Fig. 1. Schematic illustration of the alloy fabrication process using 99.9% pure Cu, Al, and Zn ingots via gravity casting, showing sequential melting and pouring at 1150°C.

casting process. After the homogenization stage, a betatizing treatment was performed at 900°C for 30 minutes, followed by cooling using two different quenching methods: DQ and UQ. Betatizing is a heat treatment intended to dissolve the material into the single beta-phase region before rapid quenching, which is a critical step in the fabrication of Cu-based SMAs. This process was carried out to control the non-diffusional transformation in the alloys. The ratio of ethanol to dry ice was controlled to achieve and maintain the mixture temperature at -5°C. The procedure began with a minimum of 800 mL of ethanol, then dry ice was added gradually until the temperature stabilized at -5°C. In the DQ method, the samples were quenched in the ethanol-dry ice medium and held for 30 minutes. In the UQ method, the samples were quenched into the ethanol-dry ice medium at -5°C for 10 minutes, then transferred to boiling water (100°C) for 30 minutes, and quenched back into the ethanol-dry ice medium at -5°C for 10 minutes.

2.3 Composition and microstructure characterization

Chemical composition analysis was performed using Optical Emission Spectroscopy (OES) to ensure that the actual composition matched the design. Microstructural analysis was conducted using an optical microscope (OM, Zeiss Primotech) and a scanning electron microscope. Samples were prepared with dimensions of approximately 10×10×5 mm³. Grinding was performed sequentially using silicon carbide papers with grit sizes of 240, 400, 600, 800, 1200, and 2000, followed by polishing with alumina 0.3 micron. Etching was carried out in a FeCl₃-ethanol solution (10 g FeCl₃ + 95 mL 95% ethanol) for 5 seconds, followed by rinsing in water. Phase identification was carried out with X-ray Diffraction (XRD, PANalytical X'Pert Pro MPD, Cu-K α). The deformation mechanism was evaluated through cold rolling using a single roll at

10% strain to observe twinning/detwinning phenomena and grain elongation.

3 Results and discussion

3.1 Chemical composition and initial microstructure of Cu-27Zn-2.5Al-(Si)

The results of the composition analysis using OES in Table 1 indicate that the alloys produced by the gravity casting process are in accordance with the design, specifically Cu-27Zn-2.5Al wt.% and Cu-27Zn-2.5Al-0.3Si wt.%. This alignment between the designed composition and the actual results indicates that the melting and homogenization processes were effective, with relatively small elemental deviations and minimal chemical segregation. One of the main challenges in fabricating Cu-Zn-Al alloys is the potential for mass loss of the Zn element due to a significant difference in melting temperature compared to Cu, which often causes compositional deviations in the final product. Therefore, the consistency between the designed composition and the experimental results shows that the melting conditions were well-controlled. This consistency is of high significance because chemical composition is a fundamental parameter that determines the phase stability and thermomechanical properties of Cu-based SMAs [1].

Table 1. Chemical composition of Cu-Zn-Al alloy

Composition (wt.%)	Cu	Zn	Al	Si	Fe	Mn
Cu-27Zn-2.5Al	Balance	27	2.5	-	<0.005	<0.001
Cu-27Zn-2.5Al-0.3Si	Balance	27	2.5	0.3	<0.003	<0.001

The microstructures of the Cu-27Zn-2.5Al and Cu-27Zn-2.5Al-0.3Si alloys are shown in Fig. 2. These observations indicate that both alloys exhibit a duplex $\alpha+\beta$ structure. The β phase forms

the matrix, while the α phase appears as a lath-shaped secondary phase. Quantitative analysis of the α -phase laths using ImageJ revealed length-to-thickness ratios (l/t) of 2.41 for Cu–27Zn–2.5Al and 2.12 for Cu–27Zn–2.5Al–0.3Si. In the Si-containing alloy, the grain size is slightly smaller than in the Si-free alloy. Based on the Cu–Zn–Al ternary diagram [12], the compositions of both alloys on the duplex $\alpha+\beta$ region. In this system, the α phase serves as a secondary phase that enhances mechanical strength, whereas the β phase forms the main matrix, capable of undergoing reversible martensitic transformation [5–6, 9]. The non-diffusional $\beta \rightarrow \beta'$ martensitic transformation is the primary mechanism responsible for the shape memory effect and super-elastic properties in Cu–Zn–Al alloys [1, 6, 13].

The microstructure in Fig. 2(b) shows that the addition of 0.3% Si does not change the dominant phase type or the morphology of the microstructure formed. However, the grain size in the alloy with the addition of Si appears finer, indicating that Si acts as a grain growth inhibitor during the solidification process. This is possible because Si atoms, which have limited solubility in the Cu lattice, can dissolve substitutionally in the matrix. The presence of Si is

also thought to slow the rate of atomic diffusion, thereby inhibiting the formation of Al- or Zn-rich secondary phase precipitates and increasing the stability of the β phase at room temperature. The results of grain size testing on samples with and without the addition of 0.3% Si are 668.26 and 415.1 microns, respectively. In Cu-based shape memory alloys, the β phase serves as the parent phase that undergoes a martensitic transformation, producing shape memory properties. The martensitic transformation in the Cu–Zn–Al system is very sensitive to compositional changes, so the addition of alloying elements, even in small amounts, can affect the thermodynamic stability of the β phase and modify the kinetics of the $\beta \rightarrow$ martensite transformation. These effects can occur through changes in lattice parameters, the formation of local strain, or modifications in the concentration of valence electrons, which collectively influence the Gibbs free energy and drive transformation [14–17]. Thus, the addition of Si to the Cu-27 Zn-2.5Al wt.% alloy has the potential to affect the characteristics of martensite transformation in the β phase, including changes in transformation temperatures such as M_s , A_s , and A_f .

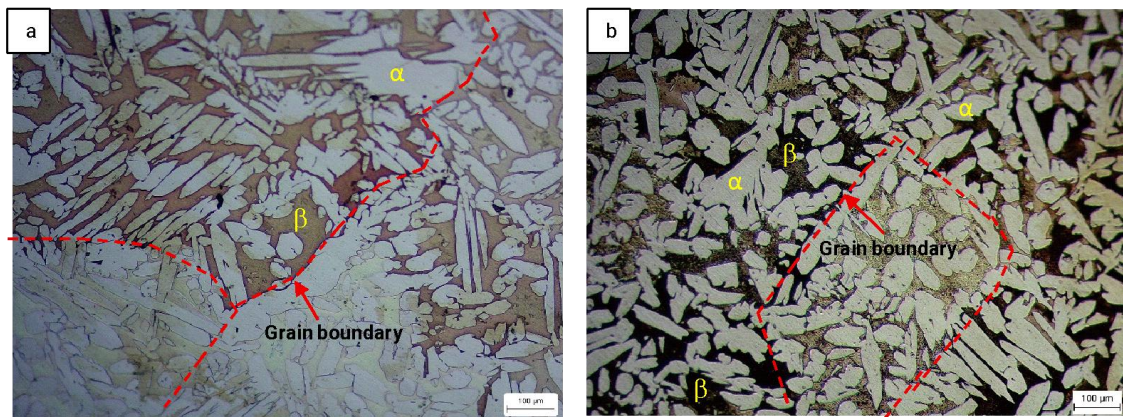


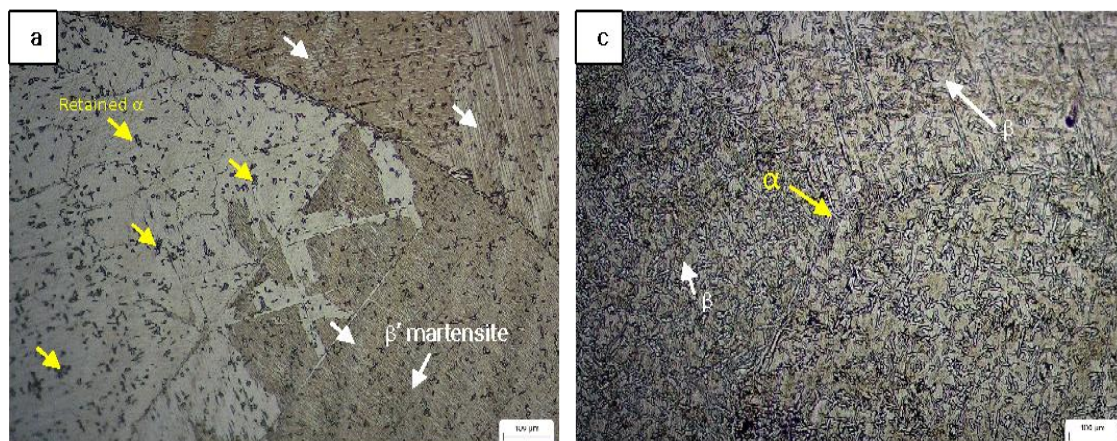
Fig. 2. Microstructure of (a) Cu–27Zn–2.5Al wt.% and (b) Cu–27Zn–2.5Al–0.3Si wt.% alloys. The β phase (BCC) as the matrix and the α phase (FCC) as the secondary phase with lath morphology.

3.2 Microstructure evolution under different quenching methods

Optical microscope observations in Fig 3.(a)–Fig. 3(d) show that variations in composition (with and without Si addition) and the DQ and UQ quenching methods have a clear effect on the phases formed after quenching. The Cu–27Zn–2.5Al wt.% alloy with both DQ and UQ methods (Fig. 3.(a)–Fig. 3(b)) is dominated by the β' martensite phase as the matrix with a needle-like morphology [6]. The β' martensite phase is formed through the nondiffusional transformation of the β phase (austenite) due to rapid cooling. In addition, the presence of retained α is identified, which is dispersed within the grains. This indicates that the alcohol medium used did not completely suppress the formation of the equilibrium α phase, so a certain amount of this phase remained stable at room temperature. Although the presence of β' martensite supports the potential for the shape memory effect, the presence of

the retained α phase has the potential to reduce the homogeneity of the reversible transformation, which is the basis for the functional properties, but it helps maintain the material's ductile properties.

In contrast, the Cu–Zn–Al–0.3Si alloy (Fig. 3(c)–Fig. 3(d)) consists of α and β phases without the formation of β' martensite. This shows that the Si element acts as a phase stabilizer by modifying the transformation free energy and strengthening the bonds within the matrix, thereby reducing the tendency for martensite formation even with a high cooling rate. This is consistent with the literature that the addition of certain elements can inhibit martensitic transformation and maintain the stability of the equilibrium phase in a metastable condition. From the microstructure analysis results, it is evident that the alloy composition and quenching method are very influential on the final phase that is formed. The addition of Si results in higher stability of the α and β phases after quenching.



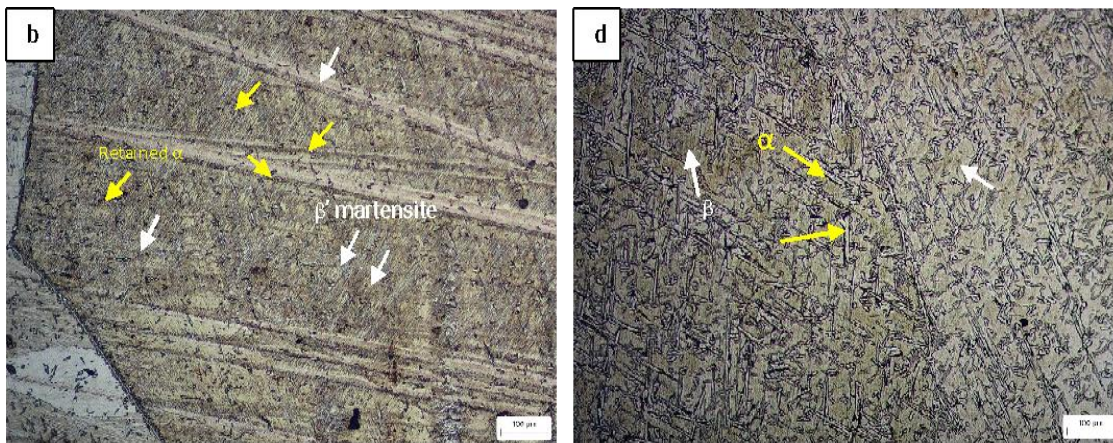


Fig. 3. Microstructure of alloys in the as-quenched condition: (a) Cu-27Zn-2.5Al wt. % _DQ; (b) Cu-27Zn-2.5Al wt. % _UQ; (c) Cu-27Zn-2.5Al-0,3 Si wt.% _DQ; (d) Cu-27Zn-2.5Al-0,3Si wt.% _UQ.

3.3 Microstructural changes and deformation mechanism after rolling

Fig. 4 shows the post-deformation microstructure of the Cu-27Zn-2.5Al wt.% alloy. It can be seen that a β' martensite phase with a V-shaped morphology was formed in the samples treated with DQ and UQ. The presence of the β' martensite phase indicates that the applied deformation has induced the transformation of the parent β phase, initially present as the matrix, into a β' martensite variant. Meanwhile, the α phase, as a secondary phase, experiences elongation after deformation and accumulates along the grain boundaries. This indirectly shows localized strain partitioning where the softer β/β' matrix accommodates martensite sliding,

while the α phase experiences stretching and plastic redistribution. This phenomenon is a non-diffusion martensite transformation, which is characteristic of SMA. When external stress is applied, the twins progressively rearrange themselves into a detwinned martensite structure. This twinning \rightarrow detwinning process produces reversible macroscopic deformation, which underlies the recoverable strain or Shape Memory Effect (SME) [1,13]. As theoretically illustrated in Fig. 4(i), the transition from twinned to detwinned martensite occurs when stress is applied, and the resulting deformation can be recovered by heating the material above its martensitic transformation temperature [13].

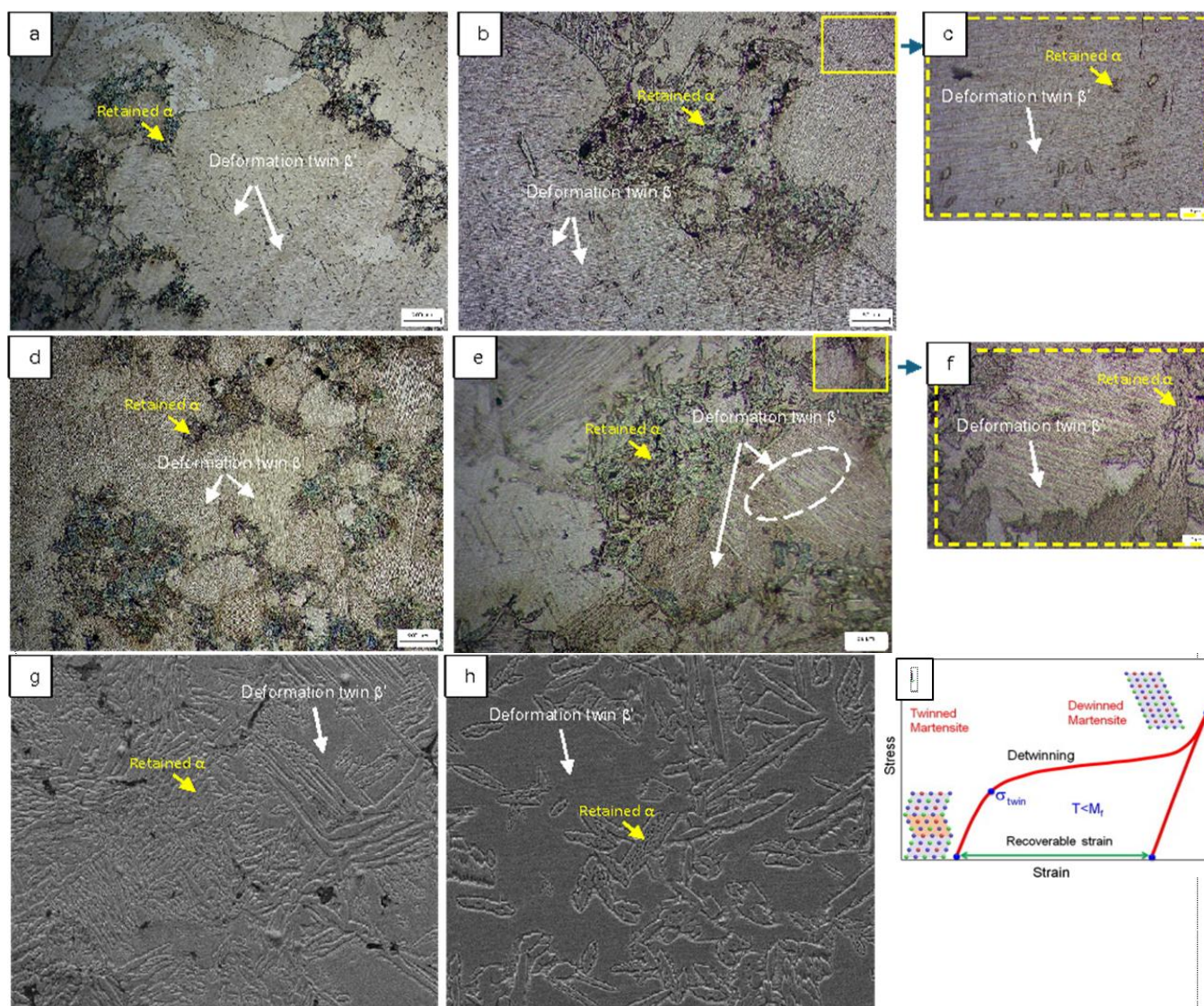


Fig. 4. Post-deformation microstructure of Cu-27Zn-2.5Al wt.% alloy in the conditions: (a-c) DQ and (d-f) UQ. (g-h) SEM images of DQ and UQ samples are shown, (i) Illustration of the martensite transformation mechanism [13].

The post-deformation microstructure of the Cu–27Zn–2.5Al–0.3Si wt.% sample is shown in Fig. 5(a)-Fig. 5(b) and reveals different deformation behaviors between the α and β phases. The α phase with its FCC crystal structure undergoes elongation, consistent with the FCC characteristic of having many active slip systems $\{111\} \langle 110 \rangle$. This configuration facilitates dislocation movement and allows plastic deformation to occur with relatively low resistance, causing the α grains to tend to elongate in morphology under loading. In contrast, the β phase with its B2 structure (ordered BCC) shows a different behavior. In the DQ sample, the β deformation shows no indication of twin formation, but rather deformation accommodated by limited slip [18]. However, in the UQ sample, the presence of deformation twins is visible in the β phase, indicating a different deformation mechanism. This phenomenon is due to crystallography and dislocations. The B2 structure has limited main slip systems on the $\{110\} \langle 111 \rangle$ and $\{112\} \langle 111 \rangle$ planes compared to FCC. If the

dislocation slip is unable to fully accommodate the deformation, twinning will occur. The role of the UQ treatment becomes very important because the reheating stage before the final quench allows for the relaxation of internal energy and improvement of ordering in the B2 lattice [9]. By reducing the density of residual defects such as stacking faults and dislocations resulting from rapid cooling, the formed β phase becomes more homogeneous and responsive. This condition increases the possibility of activating the $\{112\} \langle 111 \rangle$ twin plane when external stress is applied, making deformation twinning more likely to occur in the UQ-treated alloy. Thus, it can be concluded that the deformation mechanism in Cu–Zn–Al alloys is strongly influenced by the combination of chemical composition and the initial thermal treatment. The UQ treatment produces a β phase that is more supportive of the functional properties of SMAs, while the DQ treatment tends to produce a β phase with limited slip deformation, which is less optimal for supporting the SME.

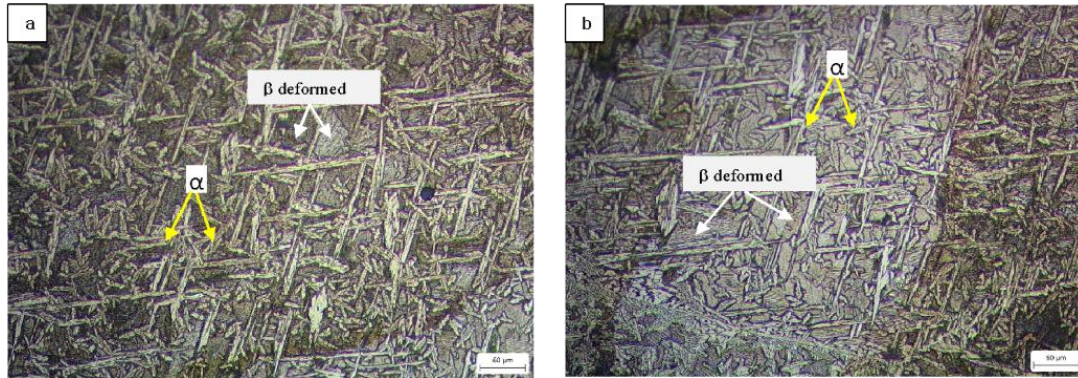


Fig. 5. Post-deformation microstructure of Cu–27Zn–2.5Al–0.3Si wt.% alloy: (a) direct quench and (b) up quench.

3.4 Phase identification

The XRD diffractograms of the Cu–27Zn–2.5Al and Cu–27Zn–2.5Al–0.3Si alloys under different conditions are presented in Fig. 6. In the as-homogenized condition (Fig. 6(a)), both alloys exhibit diffraction peaks corresponding to the α (FCC) and β (B2-BCC)

phases. The α phase is identified by its characteristic reflections with hkl (220), (111), and (112), while the β phase is represented by peaks indexed to (110) and (210). The coexistence of these phases confirms that both alloys lie within the $\alpha + \beta$ two-phase region, consistent with the Cu–Zn–Al equilibrium diagram.

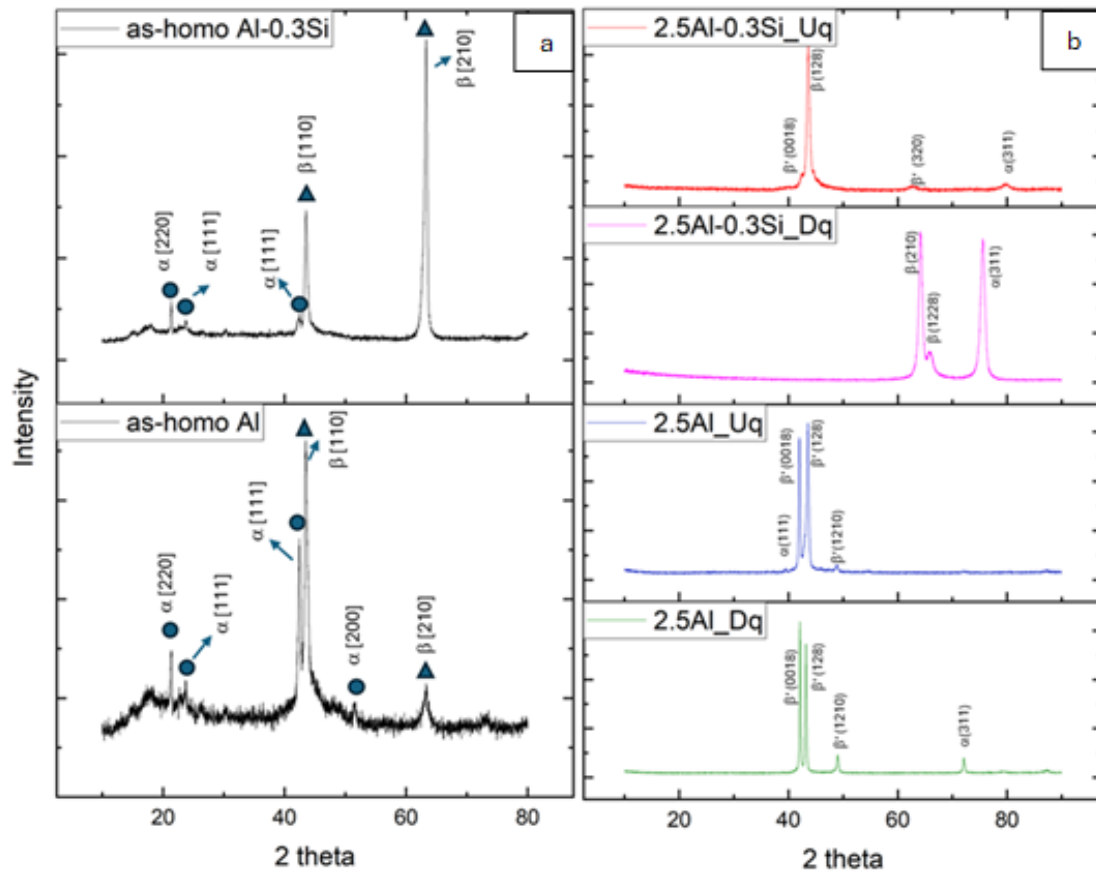


Fig. 6. XRD diffractogram of Cu–27Zn–2.5Al and Cu–27Zn–2.5Al–0.3Si wt.% alloys in (a) as-homogenized and (b) as-deformed conditions.

After deformation (Fig. 6(b)), a clear distinction is observed between the Si-free and Si-containing alloys. In the Cu–27Zn–2.5Al alloy, peaks of β' martensite are clearly visible with hkl indices such as ($\bar{1}28$), (0018/320), and (1210), indicating a thermoelastic martensitic transformation from the parent β phase. This transformation is responsible for the shape memory behavior, as it produces a reversible lattice reorientation during mechanical loading. The presence of α peaks further suggests that a small portion of the α phase remains stable during the transformation, acting as a strengthening constituent within the microstructure.

In contrast, the Cu–27Zn–2.5Al–0.3Si alloy subjected to the DQ process exhibits only α and β peaks, with no indication of β' martensite formation. This finding implies that the addition of Si suppresses the $\beta \rightarrow \beta'$ transformation by stabilizing the β phase and reducing the driving force for shear deformation. The Si atoms are believed to occupy substitutional positions within the Cu-based matrix, enhancing the lattice stability and hindering the coordinated atomic movement required for martensitic nucleation. Consequently, the alloy with Si tends to retain the equilibrium $\alpha + \beta$ structure even after deformation.

Interestingly, the Si-containing alloy treated with the UQ method exhibits weak β' martensitic peaks, suggesting a partial martensitic transformation. This phenomenon can be attributed to the intermediate reheating stage in the UQ process, which promotes atomic reordering and relieves residual stresses induced by rapid quenching. Such relaxation facilitates the formation of metastable martensite upon subsequent deformation. Therefore, it can be concluded that the Si addition and the quenching route synergistically influence the transformation behavior of Cu–Zn–Al alloys, where Si promotes phase stability. At the same time, UQ treatment partially restores the material's ability to undergo thermoelastic martensitic transformation.

4 Conclusions

This study systematically investigated the influence of quenching controlled from the α/β phase region and silicon addition on the microstructure and deformation behavior of Cu–Zn–Al-based shape memory alloys, and it can be concluded that: (1) alloys of Cu–27Zn–2.5Al and Cu–27Zn–2.5Al–0.3Si wt.% were fabricated via gravity casting, with a composition consistent with the initial design and minimal casting defects; (2) in the Cu–27Zn–2.5Al wt.% alloy, both DQ and UQ methods resulted in β' martensite after quenching. However, the UQ method promoted a higher degree of structural ordering, resulting in a more homogeneous and responsive martensitic phase; (3) the addition of 0.3 wt.% Si to Cu–27Zn–2.5Al wt.% refines the α grain and stabilizes the $\alpha + \beta$ phase, so martensite does not form after quenching; (4) the post-deformation results show that the Cu–27Zn–2.5Al wt.% alloy undergoes a twinning \rightarrow detwinning mechanism typical of SMAs, whereas in the Cu–27Zn–2.5Al–0.3Si wt.% alloy, the twinning \rightarrow detwinning mechanism was only observed in the UQ condition. The α phase dominantly undergoes plastic elongation; (5) the UQ method is prospective for controlling the formation of the β phase that supports shape memory properties, while the addition of Si plays a role in refining the microstructure but limits martensitic transformation.

Acknowledgements

This research was supported by a Fundamental Research Grant from LPPM, Universitas Pembangunan Nasional Veteran Yogyakarta, with contract No: 297/UN62/PP.01.07/KPA/2025.

References

[1] C.M. Wayman, and T.W. Duerig, "An introduction to martensite and shape memory," In *Engineering aspects of shape memory alloys*, Duerig, Ed. UK: Butterworth-Heinemann, pp. 3–20, 1990.

- [2] W. Li, S. Zuo, M. Khedr, X. Li, K. Xiong, and F. Xiao, "Microstructural mechanism underlying the stress recovery behavior of a Fe–Mn–Si shape memory alloy," *J. Mater. Res. Technol.*, vol. 30, pp. 5394–5401, 2024, doi: 10.1016/j.jmrt.2024.10.330.
- [3] Y. Gao, B. Liu, J. Tang, Z. An, and X. Zhang, "High tensile strength and shape memory effect of Ti–V–Al alloy with heterogeneous microstructure," *Mater. Sci. Eng. A*, p. 149095, 2025, doi: 10.1016/j.msea.2025.149095.
- [4] A. Setyani, I. A. Setiawan, P. R. Pamungkas, N. Sofyan, and B. T. Sofyan, "Influence of heat treatment on microstructures and shape memory effect of Cu–28Zn–2.5Al wt.% produced by gravity casting," *Int. J. Automot. Mech. Eng.*, vol. 20, no. 2, pp. 10411–10421, 2023, doi: 10.15282/ijame.20.2.2023.07.0805.
- [5] A. Setyani, A. Novakusuma, B. T. Sofyan; Optimisation of heat treatments on shape memory effect of Cu–24Zn–3.65Al wt. % alloy produced by gravity casting. *AIP Conf. Proc.* 21 July 2023; 2689 (1): 070046. <https://doi.org/10.1063/5.0114835>
- [6] V. Asanovic, D. Radonjic, J. Scepanovic, and D. Vuksanovic, "Effect of chemical composition and quenching media on recoverable strain in Cu–Zn–Al alloys," *Journal of Materials Research and Technology*, vol. 12, pp. 1368–1379, 2021. <https://doi.org/10.1016/j.jmrt.2021.03.098>
- [7] G. Guénin, "Martensitic transformation and thermomechanical properties," *Key Engineering Materials*, vols. 101–102, pp. 339–392, 1995, doi: 10.4028/www.scientific.net/KEM.101-102.339
- [8] F. Dagdelen, M. S. Kanca, and M. Kok, "Effects of different quenching treatments on thermal properties and microstructure in quaternary Cu-based HTSMA," *Phys. Met. Metallogr.*, vol. 120, no. 13, pp. 1378–1383, 2019, doi: 10.1134/S0031918X1913009.
- [9] A. Setyani, I.A. Setiawan, D.R.K. Pertiwi, and B.T. Sofyan, "Effects of quenching methods on shape memory properties of Cu–28Zn–3Al wt. % alloy produced by gravity casting," *Indian Journal of Engineering & Materials Sciences*, vol. 29, pp. 100–107, 2022. DOI: 10.56042/ijems.v29i1.46040
- [10] S. Longauer, M. Votjko, G. Janak, and M. Longauerova, "Stabilization of martensite in also microstructure of a Cu–Zn–Al shape-memory alloy," *Journal de Physique IV France*, vol. 112, pp. 523–527, 2003. DOI: 10.1051/jp4:2003939
- [11] N. M. Lohan, M.G. Suru, B. Pricop, and L.G. Bujoreanu, "Cooling rate effects on the structure and transformation behavior of Cu–Zn–Al shape memory alloys," *International Journal of Minerals, Metallurgy and Materials*, vol. 21, no. 11, pp. 1109–1114, 2014. <https://doi.org/10.1007/s12613-014-1015-5>
- [12] S-M. Liang, and S-F. Rainer, CALPHAD: Computer coupling of phase diagrams and thermochemistry thermodynamic assessment of the Al – Cu – Zn system, Part III: Al – Cu – Zn ternary system. *Calphad*, 2016; 52: pp. 21–37. DOI: 10.1016/j.calphad.2015.11.001
- [13] K. K. Alaneme, J. U. Anaele, and E. A. Okotete, "Martensite aging phenomena in Cu-based alloys: Effects on structural transformation, mechanical and shape memory properties: A critical review," *Sci. Afr.*, vol. 12, p. e00760, 2021, doi: 10.1016/j.sciaf.2021.e00760.
- [14] X. Chen, Y. Wang, Z. Li, and Q. Meng, "Thermodynamics and characterization of shape memory Cu–Al–Zn alloys," *Trans. Nonferrous Met. Soc. China*, vol. 25, no. 8, pp. 2630–2636, Aug. 2015, doi: 10.1016/S1003-6326(15)63884-3.
- [15] E. M. Mazzer, M. R. da Silva, and P. Gargarella, "Revisiting Cu-based shape memory alloys: Recent developments and new perspectives," *J. Mater. Res.*, vol. 37, pp. 162–182, 2022, doi: 10.1557/s43578-021-00444-7

- [16] F. J. Gil, and J.M. Guilemany, "The determination of the influence of heat treatment on the martensitic transformation in Cu Zn-Al-Mn shape-memory alloy by calorimetry and acoustic emission techniques," *Thermochimica Acta*, vol. 205, pp. 75–85, 1992. [https://doi.org/10.1016/0040-6031\(92\)85250-Y](https://doi.org/10.1016/0040-6031(92)85250-Y)
- [17] N. Kayali, S. Ozgen, and O. Adigiizel, "The influence of ageing on martensite morphology in shape memory CuZnAl alloys," *J. Phys. IV France*, vol. 7, no. C5, pp. C5-317–C5-322, 1997. DOI: 10.1051/jp4:1997550
- [18] A. Cuniberti, R. Romero, and A. Condó, "Compression-induced hexagonal martensite in Cu-Zn-Al," *Materials Science and Engineering A*, vol. 325, no. 1–2, pp. 177–181, 2002. [https://doi.org/10.1016/S0921-5093\(01\)01443-5](https://doi.org/10.1016/S0921-5093(01)01443-5).